Inorganic Chemistry

ARTICLE

pubs.acs.org/IC

# Examples of Reductive Azo Cleavage and Oxidative Azo Bond Formation on $Re_2(CO)_{10}$ Template: Isolation and Characterization of Re(III) Complexes of New Azo-Aromatic Ligands

Nanda D. Paul,[†] Subhas Samanta,[†] Tapan K. Mondal,[‡] and Sreebrata Goswami*[,†]

[†]Department of Inorganic Chemistry, Indian Association for the Cultivation of Science, Jadavpur, Kolkata 700 032, India

[‡]Department of Chemistry, Jadavpur University, Jadavpur, Kolkata 700 032, India

Supporting Information

**ABSTRACT:** A new example of simultaneous reductive azo bond cleavage and oxidative azo bond formation in an azo-aromatic ligand is introduced. The chemical transformation is achieved by the reaction of $Re_2(CO)_{10}$ with the ligand 2-[(2-N-Arylamino)phenylazo]pyridine ($HL^1$). A new and unexpected mononuclear rhenium complex $[Re(L^1)(L^3)]$ (**1**) was isolated from the above reaction. The new azo-aromatic ligand, $H_2L^3$ ($H_2L^3$ = 2, 2′-dianilinoazobenzene) is formed in situ from $HL^1$. A similar reaction of $Re_2(CO)_{10}$ and a closely related azo-ligand, 2,4-ditert-butyl-6-(pyridin-2-ylazo)-phenol ($HL^2$), resulted in a seven coordinated compound $[Re(L^2)\{(L^4)^{\bullet-}\}_2]$ (**2**; $HL^4$ = 2-amino-4,6-ditert-butyl-phenol) *via* reductive cleavage of the azo bond. The complexes have been characterized by using a host of physical methods: X-ray crystallography, nuclear magnetic resonance (NMR), cyclic voltammetry, ultraviolet−visible (UV−vis), electron paramagnetic resonance (EPR) spectroscopy, and density functional theory (DFT). The experimental structures are well reproduced by density functional theory calculations and support the overall electronic structures of the above compounds. Complex **1** is a closed shell singlet, while complex **2** exemplifies a singlet diradical complex where the two partially oxidized aminophenoleto ligands are coupled to each other, yielding the observed diamagnetic ground state. Complexes **1** and **2** showed two successive one-electron redox responses. EPR spectral studies in corroboration with DFT results indicated that all of the redox processes occur at the ligand center without affecting the trivalent state of the metal ion.

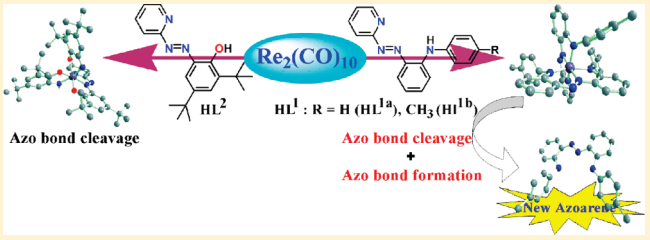


## INTRODUCTION

Metathesis reactions[1] in unsaturated organic molecules constitute an important class of chemical reactions that occur with simultaneous bond cleavage and bond formation processes. Accordingly, metathesis in olefins has gained widespread use in research and industry for making products ranging from medicines and polymers to enhanced fuels.[1,2] In comparison, such a reaction in azo compounds is not known. Diazo compounds, in general, and azo-aromatics, in particular, are high-value chemicals widely used in industry as organic dyes, indicators, pigments, food additives, radical reaction initiators, and therapeutic agents.[3]

In recent times, we have been in search[4] of synthetic protocols suitable for the isolation of transition metal complexes of azo-anion radical ligands. In this respect, zerovalent metal carbonyl complexes were found[4a−c] to be useful precursors where the electron-rich metal center acts as a possible electron pool. Following this synthetic protocol, we have been successful in isolation of stable complexes of azo-anion radical ligands. The ligands containing azo functions are known to undergo reduction[4−6] chemically or electrochemically at rather accessible potentials to form stable azo-anion radicals (−1) or dianionic hydrazido (−2) species. The further addition of two more electrons to a hydrazido function leads to the rupture[7] of the N−N bond (Scheme 1).

**Scheme 1. Electron Transfer Series**

$$[-N{=}N-]^{0} \underset{-e}{\overset{+e}{\rightleftharpoons}} [-N^{\bullet-}\cdots N-]^{-} \underset{-e}{\overset{+e}{\rightleftharpoons}} [-\tilde{N}-\tilde{N}-]^{2-} \underset{-2e}{\overset{+2e}{\rightleftharpoons}} 2[-N]^{2-}$$

With this available knowledge, we set out to explore the chemical reactions of $Re_2(CO)_{10}$ with the two extended tridentate azoaromatic ligands, $HL^1$ and $HL^2$ (Scheme 2), that are known to undergo facile reduction and produce stable azo-anion radical complexes.[4] In practice, the reference chemical reaction with $HL^1$ produced a Re compound $[Re(L^1)(L^3)]$ (**1**) of a newly formed azoaromatic ligand $H_2L^3$ (Schemes 3 and 4). The formation of $H_2L^3$ from $HL^1$ is noteworthy and proceeds *via* simultaneous azo bond cleavage and N−N bond fusion reactions. However, a similar reaction with $HL^2$ (Scheme 3) and $Re_2(CO)_{10}$ led only to the reductive cleavage of the azo function with the formation of a complex of a 2-aminophenol derivative, $[Re(L^2)\{(L^4)^{\bullet-}\}_2]$ (**2**; Scheme 4). Notably, metal mediated azo bond cleavage[7] leading to the imido complexes has long been

**Received:** June 4, 2011
**Published:** July 20, 2011

**Scheme 2. Ligands: Reactants**

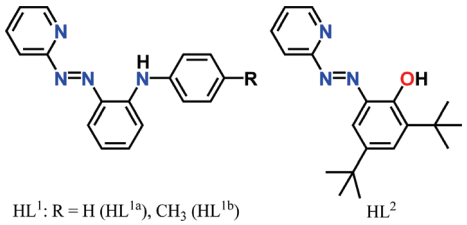


$HL^1$: R = H ($HL^{1a}$), $CH_3$ ($HL^{1b}$) $HL^2$

**Scheme 3. Reactions**

$Re_2(CO)_{10}$ + $HL^1$ $\xrightarrow{\text{n-octane/reflux}}$ $[Re(L^1)(L^3)]$ (1) + other products

$Re_2(CO)_{10}$ + $HL^2$ $\xrightarrow{\text{n-octane/reflux}}$ $[Re(L^2)(L^{4\bullet-})_2]$ (2) + other products

known in the literature, but unification of metal-imido fragments to azo arene *via* N−N coupling reactions is scarce.[8] And these two reactions occurring together in a single chemical reaction, as happened here, is nonexistent in the literature.

## RESULTS AND DISCUSSION

**Syntheses and Characterization.** The ligand, $HL^1$, offers three very different kinds of coordination atoms, namely, a pyridyl-N, a reducible azo function containing N, and a diarylamido-N (N, after deprotonation), whereas the ligand $HL^2$ is very similar to the previous one where the secondary amide-N is replaced by a phenolate group (Scheme 2). Pyridyl-N and azo-N are $\pi$ accepting, whereas deprotonated amido-N and phenolate-O ligands are strongly donating.

The reactions of $Re_2(CO)_{10}$ (0.15 mmol) with $HL^1$ (0.60 mmol) in boiling *n*-octane produced new reddish pink $[Re(L^1)(L^3)]$ complexes (**1a** and **1b**) in 45 and 43% yield, respectively (Scheme 3). While selecting Re(0)-carbonyl as the starting compound, it was anticipated that the substitution of CO ligands by $[L^1]^-$ with concomitant internal electron transfer from the electron-rich metal Re(0) to the reducible azo aromatic ligand $[L^1]^-$ would produce the metal radical complex directly.[4a−c] However, the reference reaction produced a totally unexpected product. The compound, isolated from the reaction mixture, contained an undissociated tridentate ligand $[L^1]^-$ and a new dianionic azo-aromatic ligand $[L^3]^{2-}$ coordinated in a tridentate fashion. Formation of the new ligand $[H_2L^3]$ is noteworthy, which involves simultaneous reductive azo bond cleavage and N−N bond formation. These results immediately prompted us to explore a similar reaction of $Re_2(CO)_{10}$ with another extended azo-aromatic ligand. We purposefully chose $HL^2$ for carrying out the reaction, as its conjugate base offers a nearly similar coordination environment like $[L^1]^-$. The reaction of $HL^2$ and $Re_2(CO)_{10}$, under identical reaction conditions, however, formed a seven coordinated mixed ligand complex $[Re(L^2)\{(L^4)^{\bullet-}\}_2]$ (**2**) in nearly 60% yield (Schemes 3 and 4). In this compound, two partially oxidized (semiquinone) aminophenolato ligands ($L^{4\bullet-}$) are coordinated along with an undissociated $[L^2]^-$ ligand. 2-Aminophenoleto ligands are formed in situ *via* the reductive cleavage of the parent $[L^2]^-$ ligand. The above chemical reactions also produced several low-yield byproducts, as seen on a preparative TLC plate, which could not be purified so far. It may be worth noting that seven coordinated complexes of Re are rare.[9]

**Scheme 4. Ligands: Products**

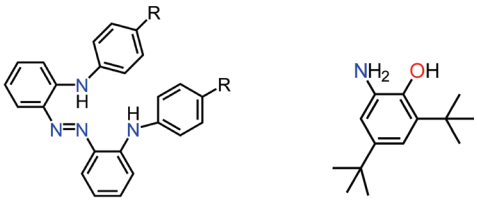


$H_2L^3$: R = H ($H_2L^{3a}$), $CH_3$ ($H_2L^{3b}$) $H_2L^4$

The complexes, **1** and **2**, gave satisfactory elemental analyses (*cf.*, Experimental Section). Electrospray mass spectra of the complexes corroborate their formulation as $[Re(L^1)(L^3)]$ (**1**) and $[Re(L^2)(L^4)_2]$ (**2**), respectively. For example, each of the complexes **1a** and **2** showed an intense peak due to the respective molecular ion $[\mathbf{1a}\text{-}H]^+$ and $[\mathbf{2}\text{-}H]^+$ at $m/z$ 822 and 936 amu, respectively. Notably, the experimental spectral features of the complexes corroborate very well with their simulated isotopic pattern for the given formulation. Representative spectra of **1a** and **2** along with their simulations are in the Supporting Information, Figures S1 and S2.

Complexes **1** and **2** possess $S = 0$ ground states, as determined by magnetic susceptibility measurements at room temperature. They display sharp $^1H$ NMR signals in the normal range[10] for diamagnetic compounds. The $^1H$ NMR spectra of the representative complexes are submitted as Supporting Information, Figures S3−S5. Notably, the protons in the mixed ligand complexes **1** and **2** are unique and displayed a very large number of resonances. There has been serious overlap of resonances of the aromatic region, and it was not possible to assign them. However, complex **1b** showed three methyl proton resonances at $\delta$ 1.99, 2.19, and 2.32 ppm. The two imine N−H protons of **2** appeared at $\delta$ 8.98 and 9.32 ppm, respectively, which disappeared on $D_2O$ shake.

**Rationale for the Transformation $HL^1 \rightarrow H_2L^3$.** The reaction of $Re_2(CO)_{10}$ with $HL^1$ exemplifies an unprecedented chemical reaction wherein a dianionic tridentate N,N,N donor ($H_2L^3$) is formed *via* simultaneous four electron reductive cleavage and oxidative recombination of the aryl imides. The conversion $HL^1 \rightarrow H_2L^3$ occurs within the coordination sphere, and the overall reaction is a multiple electron transfer process where the electron-rich dimetallic $Re_2(CO)_{10}$ serves as an electron pool.

The mechanisms of these chemical reactions are not resolved as yet. However, a few reactions have been planned, and the results along with related literature have been used to make a reasonable assessment of the reference reaction. It has been argued[7a,11] before that both reductive azo cleavage as well as oxidation of the coordinated organo-imides to a diazo function are facilitated by the dimetallic mediators. For example, an oxidative N−N bond formation reaction in a Ta complex has been achieved recently in a bridging imido dimer.[8] For comparison, in the present case, the zero-valent $Re_2$ complex has mediated the two opposite redox processes, reductive bond cleavage as well as oxidative azo bond fusion, simultaneously. It is worth noting here that the reactions of the monomeric $Re(CO)_5Cl$ with $HL^1$ under identical conditions failed to bring


dx.doi.org/10.1021/ic201200r |*Inorg. Chem.* 2011, 50, 7886–7893

**Scheme 5. Summary of Ligand Transformations**

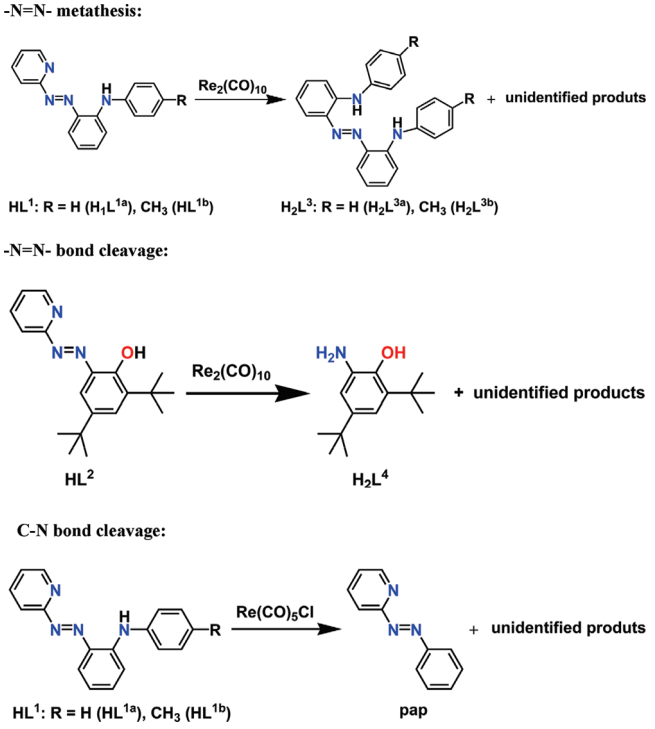


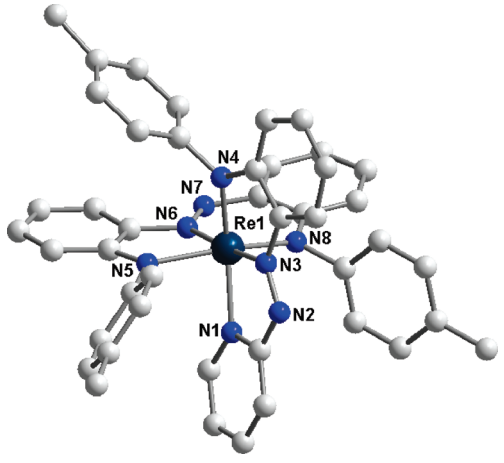


**Figure 1.** Molecular view of **1b**. Hydrogen atoms are omitted for clarity.

about similar transformation. The latter reaction produced $[Re(pap)(CO)_3Cl]$ (**3**) (pap =2-(phenylazo)pyridine, N^\N) as the only isolable product (cf. Experimental Section).[12] The formation of pap from $HL^1$ *via* deamination[4c] has been observed previously in several other reactions. The three-dimensional X-ray structure (ORTEP) of compound **3** is submitted as Supporting Information Figure S6. In contrast, a similar reaction of $HL^2$ with $Re_2(CO)_{10}$ stopped after the cleavage of the azo bond, producing amino phenol from $HL^2$. We wish to note here that the two coordinated nitrogen atoms of the two amino phenolato ligands in compound **2** are disposed in *trans* orientations, which is not a favorable geometry for an interligand recombination reaction for N−N bond formation. Moreover, the reactions of closely related bidentate azo-aromatic ligands,

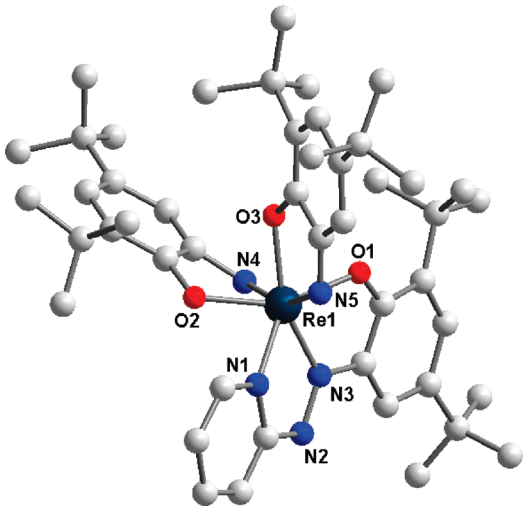


**Figure 2.** Molecular view of **2**. Hydrogen atoms are omitted for clarity.

like pap or 4-aryl substituted pap (N^\N) ($L^5$) with $Re_2(CO)_{10}$ (see Experimental Section) under identical reaction conditions, underwent substitution and electron transfer, producing a diradical complex, $[Re^{II}(N^{\wedge}N^{\bullet-})_2(CO)_2]$.[4a] To exclude the possibility of the formation of $H_2L^3$ *via* multiple oxidative bond fusion of aromatic mono amine, produced *via* deamination of $HL^1$, a reaction with the −Me substituted ligand $HL^{1b}$ (Scheme 2) was carried out. Interestingly, the product obtained from this reaction contains the new ligand $H_2L^{3b}$, which is symmetrical about the azo function. All of these observations taken together suggest that $HL^1 \rightarrow H_2L^3$ conversion occurs *via* a sort of overall azo bond metathesis. However, the other metathesis product could not be identified so far. The observed ligand transformations in the present work are summarized in Scheme 5.

**X-Ray Crystal Structure.** The complexes **1b** and **2** form good quality crystals, whose structures have been solved by single-crystal X-ray diffraction studies. Molecular views of the compounds **1b** and **2** are displayed in Figures 1 and 2, respectively. Crystallographic data and selected experimental as well as DFT computed structural parameters are listed in Tables 1−3; ORTEPs are submitted as Supporting Information (Figures S7 and S8).

The X-ray structure of **1b** indeed confirmed the formation of $H_2L^3$ from $HL^1$. Complex **1b** is hexa-coordinated and is meridional. The two deprotonated ligands, $[L^{1b}]^-$ and $[L^{3b}]^{2-}$, coordinate the central rhenium ion in an $N_6$-fashion using pairs of pyridyl-N, azo-N, and amido-N (deprotonated secondary amine) atoms. The chelate bite angle of N(pyridyl)−Re−N(azo) (73.57(5)°) is smaller than the average of N(azo)−Re−N(amide) (81.83(6)°).[10] The crystal structure of compound **2**, on the other hand, is hepta-coordinated.[9] An anionic tridentate ligand $[L^2]^-$ and two bidentate amino phenolato ligands $(HL^4)^-$ complete the coordination environment about the central Re atom. The ligand $[HL^4]^-$ is formed *via* reductive cleavage of the azo bond in $HL^2$. Its coordination geometry is distorted pentagonal bipyramidal, and the rhenium atom sits in a basal plane formed by O1, O2, O3, N1, and N3 atoms. The axial positions are occupied by N4 and N5 atoms (N4−Re1−N5 angle is 160°) (Figure 2) of the two $[HL^4]^-$ ligands. Notably, the two nitrogen atoms of the amino phenolate ligands are disposed *trans* to each other. We wish to note here that the average $d_{(N-N)}$ lengths of

**Table 1. Crystallographic Data for 1b, 2, and 3**

| | 1b | 2 | 3 |
|---|---|---|---|
| empirical formula | $C_{44}H_{37}N_8Re$ | $C_{47}H_{66}N_5O_3Re$ | $C_{14}H_9ClN_3O_3Re$ |
| molecular mass | 864 | 963.27 | 488.90 |
| temp (K) | 150 K | 150 K | 150 K |
| cryst syst | monoclinic | triclinic | monoclinic |
| space group | $P21/c$ | $P\bar{1}$ | $P21/n$ |
| $a$ (Å) | 9.7491(3) | 10.579(6) | 12.4199(19) |
| $b$ (Å) | 19.0490(6) | 12.786(7) | 9.0921(14) |
| $c$ (Å) | 21.1424(6) | 18.829(11) | 13.818(2) |
| α (deg) | 90 | 94.595(14) | 90 |
| $\beta$ (deg) | 100.0780(10) | 92.864(16) | 102.650(5) |
| $\gamma$ (deg) | 90 | 102.871(14) | 90 |
| $V$ (Å$^3$) | 3865.8(2) | 2469(2) | 1522.5(4) |
| $Z$ | 4 | 2 | 4 |
| $D_{calcd}$ (g/cm$^3$) | 1.630 | 1.296 | 2.133 |
| cryst dimens (mm) | 0.08 × 0.16 × 0.18 | 0.15 × 0.17 × 0.19 | 0.08 × 0.16 × 0.18 |
| $\theta$ range for data collection (deg) | 1.5−28.6 | 1.1−24.7 | 2.0−24.3 |
| GOF | 1.01 | 1.03 | 1.01 |
| reflns collected | 43806 | 26869 | 16378 |
| unique reflns | 9605 | 8364 | 2484 |
| final $R$ indices [$I > 2\sigma(I)$] | R1 = 0.0338 | R1 = 0.0599 | R1 = 0.0322 |
| | wR2 = 0.0714 | wR2 = 0.1668 | wR2 = 0.0702 |

**Table 2. Summary of Selected Experimental and Calculated Bond Lengths (Å) of Complexes 1b, $[1b]^+$, and $[1b]^{2+}$**

| | 1b | | $[1b]^+$ | $[1b]^{2+}$ |
|---|---|---|---|---|
| bonds | X-ray | theoretical | theoretical | theoretical |
| Re1−N(1) | 2.076(3) | 2.101 | 2.109 | 2.120 |
| Re1−N(3) | 1.972(3) | 1.990 | 2.020 | 2.073 |
| Re1−N(4) | 1.957(3) | 2.012 | 1.992 | 1.976 |
| Re1−N(5) | 1.977(3) | 2.008 | 2.038 | 2.116 |
| Re1−N(7) | 2.037(3) | 2.077 | 2.062 | 2.047 |
| Re1−N(8) | 2.081(3) | 2.131 | 2.100 | 2.028 |
| N(2)−N(3) | 1.336(5) | 1.322 | 1.306 | 1.286 |
| N(6)−N(7) | 1.330(5) | 1.296 | 1.304 | 1.316 |
| C(35)−N(8) | 1.402(5) | 1.400 | 1.382 | 1.343 |

**Table 3. Summary of Selected Experimental and Calculated Bond Lengths (Å) of Complexes 2, $[2]^+$, and $[2]^{2+}$**

| | 2 | | $[2]^+$ | $[2]^{2+}$ |
|---|---|---|---|---|
| bonds | X-ray | theoretical | theoretical | theoretical |
| Re1−O1 | 2.016(6) | 2.069 | 2.063 | 2.024 |
| Re1−O2 | 1.976(6) | 2.081 | 2.118 | 2.132 |
| Re1−O3 | 2.047(6) | 2.035 | 2.091 | 2.113 |
| Re1−N1 | 2.066(8) | 2.098 | 2.131 | 2.159 |
| Re1−N3 | 2.020(8) | 2.047 | 2.087 | 2.121 |
| Re1−N4 | 1.990(7) | 2.035 | 2.087 | 2.077 |
| Re1−N5 | 1.971(8) | 2.019 | 2.052 | 2.076 |
| C25−O2 | 1.350(12) | 1.325 | 1.301 | 1.291 |
| N2−N3 | 1.347(11) | 1.325 | 1.312 | 1.301 |
| C20−N4 | 1.353(11) | 1.365 | 1.340 | 1.326 |
| C20−C25 | 1.378(14) | 1.428 | 1.445 | 1.469 |
| C21−C22 | 1.392(16) | 1.386 | 1.375 | 1.372 |
| C23−C24 | 1.389(16) | 1.392 | 1.379 | 1.374 |
| C39−O3 | 1.332(11) | 1.337 | 1.309 | 1.298 |
| C34−N5 | 1.361(12) | 1.364 | 1.347 | 1.327 |
| C34−C39 | 1.435(12) | 1.418 | 1.441 | 1.464 |
| C35−C36 | 1.366(14) | 1.388 | 1.377 | 1.371 |
| C37−C38 | 1.409(13) | 1.394 | 1.374 | 1.371 |

the azoaromatic ligands in both the compounds **1b** and **2** are elongated (for **1b**, 1.333(5); **2**, 1.347(11)Å) compared to the uncoordinated ligand salt,[13] $[HL^{1a}]ClO_4$ (1.246(5)Å). The elongation of the −N═N− chromophores in these complexes is due to extensive Re(d$\pi$)-ligand($\pi^*$) back-bonding,[10,14] which has been supported by DFT studies. However, the two aminophenolates in complex **2** are partially oxidized: the C−N and C−O lengths are in agreement with the bond lengths in its semiquinone oxidation state.[15] Ambiguities of oxidation states in the above coordinated azo-aromatics have been finally sorted out by their DFT analysis (cf. below).

The metal−nitrogen bonds in these complexes are unexceptional, lying in the range 1.95−2.07 Å. The bonds from Re to the neutral 2-pyridyl-N atoms are distinctly longer than those to the anilido or azo nitrogen atoms.[10,14] The effects of the −N═N− bond elongation due to back bonding are also reflected by the lowering of vibrational frequencies of $\nu_{N=N}$ as compared to the uncoordinated $HL^1/HL^2$. For example, the $\nu_{N=N}$ band in free ligands appears near 1380 cm$^{-1}$, whereas it is lowered considerably in the coordinated states and appeared at 1285 and 1260 cm$^{-1}$ in the complexes **1a** and **2**, respectively.[13,16]

**Cyclic Voltammetry and EPR.** Cyclic voltammograms of **1a**, **1b**, and **2** were recorded in $CH_2Cl_2$ solutions containing 0.1 M TBAP at 25 °C. The potentials are referenced to the saturated


dx.doi.org/10.1021/ic201200r |Inorg. Chem. 2011, 50, 7886–7893

**Table 4. Electrochemical Data**[a]

| compound | oxidation $E_{1/2}$,[b] V ($\Delta E_p$, mV) |
|---|---|
| $[Re(L^{1a})(L^{3a})]$ (**1a**) | 0.43 (80), 0.82 (70) |
| $[Re(L^{1b})(L^{3b})]$ (**1b**) | 0.41 (75), 0.79 (80) |
| $[Re(L^{2})(L^{4\bullet-})_2]$ (**2**) | 0.53 (75), 0.10 (80) |

[a] Conditions: solvent, dichloromethane; supporting electrolyte, $NBu^t_4ClO_4$ (0.1M); working electrode, platinum for oxidation and reduction processes; reference electrode, Ag/AgCl; solute concentration, *ca.* $10^{-3}$(M); scan rate, 50 $mVs^{-1}$. [b] $E_{1/2} = 1/2(E_{pa}+E_{pc})$, $\Delta E_p = E_{pa} - E_{pc}$ in mV ($E_{pa}$ = anodic peak potential, $E_{pc}$ = cathodic peak potential).

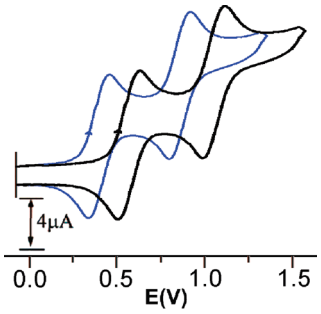


**Figure 3.** Cyclic voltammogram of **1** and **2** in $CH_2Cl_2$.

Ag/AgCl electrode. The results are summarized in Table 4, and the voltammograms (for **1a** and **2**) are displayed in Figure 3. Both complexes **1** and **2** showed two reversible anodic responses in the potential range 0.3−1.0 V. One-electron stoichiometry of the reversible redox processes was confirmed by exhaustive electrolyses of the representative compounds **1a** at 0.65 and 1.0 V and **2** at 0.7 and 1.2 V, respectively.

To have an insight into the nature of the electronic levels associated with the reversible redox processes, electrogenerated complexes were studied by EPR spectroscopy in $CH_2CL_2$/0.1 M TBAP at 77 K. The one electron oxidized complexes $[\mathbf{1a}]^+$ and $[\mathbf{2}]^+$, generated by exhaustive electrolysis of [**1a**] and [**2**] at 0.65 and 0.7 V, respectively, displayed ligand-centered sharp single line spectra at $g = 2.006$ and $g = 2.003$, respectively, with peak to peak line widths of 308 mT to 343 mT, which indicate that each of the oxidized complexes undergoes ligand based oxidation, and consequently the unpaired spin is localized primarily on the coordinated ligand.[4,15] The two electron oxidized dipositive compounds, $[\mathbf{1}]^{2+}$ and $[\mathbf{2}]^{2+}$, are, however, EPR silent, as expected. EPR spectra of all of the above one electron oxidized complexes are displayed in Figure S9 of the Supporting Information. These results are fully corroborated by density functional theory (DFT) calculations, which show that the highest occupied molecular orbitals (HOMO, HOMO−1) of the complexes **1b** and **2** are primarily ligand-centered (cf. below). Thus, one electron oxidation in these complexes is expected to occur from the ligand centers and produce monocationic ligand-centered radical complexes of Re(III), as observed experimentally.

**The Electronic Structures and UV−Vis Spectra.** Because of the redox noninnocent nature of the coordinated ligands, the assignment of electronic structures of these complexes is an important issue in view of different electronic structure possibilities[4,15] (Schemes 1 and 6). In order to have a definite look into the electronic structures of these two complexes **1** and **2**, the geometries of the complexes **1b** and **2** in both singlet and triplet states were optimized, using density functional theory (B3LYP and SDD on Re; 6-31+G(d) on C, N, and O; 6-31G on H atoms—see Experimental Section). The agreement between the experimental structural parameters and that obtained through DFT calculations for **1b** and **2** were found to be excellent. Calculated selected bond lengths and angles are compared with experimental ones in Tables 2 and 3.

**Scheme 6. Different Electronic Possibilities of $H_2L^4$**

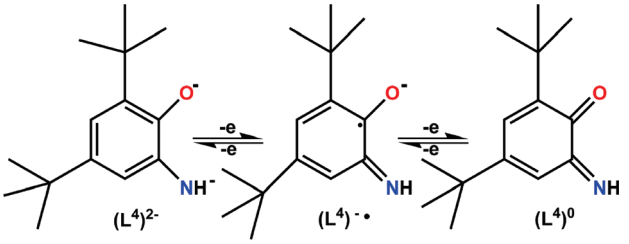


The most stable structure of **1b** proves to be a closed-shell singlet state, $[Re^{III}(L^{1b})(L^{3b})]$, and all attempts to locate open-shell singlet $[Re^{V}(L^{1b})^{\bullet-}(L^{3b})^{\bullet-}]$ configurations using the BS-DFT approach converged back to the closed-shell configuration. Complex **2**, on the other hand, on broken symmetry density functional theoretical calculations (BS ($S = 0$)), clearly shows that the two aminophenoleto ligands ($L^4$) are open-shell, $\pi$-radical monoanions $[(L^4)^{\bullet-}]$, as was shown computationally for the analogous systems.[15] The sensitive bond distances associated with the coordinated $L^4$ (C−O and C−N X-ray bond distances) and NBO calculated average Wiberg bond order (C−O, 1.138 (1.151 and 1.125) and C−N, 1.223 (1.229 and 1.219)) in complex **2** suggests its intermediate semiquinone $[(L^4)^{\bullet-}]$ radical state leading to the valence configuration of $[Re^{III}(L^2)^-\{(L^4)^{\bullet-}\}_2]$. Notably, one of these two ligands remains in the spin-up manifold, while the second one is in the spin-down manifold, yielding the observed antiferromagnetically coupled diamagnetic singlet ($S = 0$) ground state. This notion is further confirmed by the Mulliken spin population analysis (Figure S10, Supporting Information) and is very similar to the results calculated for similar systems.[15] The elongation of the azo-chromophores in both complexes **1** and **2** is due to substantial $d\pi(Re)\rightarrow\pi^*(N{=}N)$ back bonding, which indeed is consistent with the substantially reduced Wiberg index for the N−N bonds (1.33 and 1.41 for **1b**, 1.29 for **2**) compared to the free-ligand value of 1.77.[14]

The energies and compositions of the DFT calculated frontier orbitals for both complexes, $[Re(L^{1b})(L^{3b})]$ (**1b**) and $[Re^{III}(L^2)\{(L^4)^{\bullet-}\}_2]$ (**2**), are listed in the Supporting Information (Tables S1 and S2). For both complexes **1b** and **2**, the MO representations show the highest occupied MO (HOMO) to be formed by a combination of d metal orbitals and ligand orbitals with a major contribution from the ligand orbitals (**1b**: $L^{1b}$, 05%; Re, 09%; $L^{3b}$, 86% and **2**: $L^2$, 11%, Re, 04%; $L^4$, 85%). Closely lying occupied HOMO−1 is again formed by a major contribution of ligand orbitals. The lowest lying unoccupied MOs (LUMOs) are, to a large extent, delocalized over the $\pi$ system of the ligands; metal orbitals contribute to this orbital only by a very little amount (Tables S1 and S2, Supporting Information).

Geometry optimizations were also carried out on the one- and two-electron oxidized redox partners of **1b** and **2**. Optimized


dx.doi.org/10.1021/ic201200r |*Inorg. Chem.* 2011, 50, 7886–7893

**Table 5. UV−Vis−NIR Spectral Transition of the Complexes 1 and 2**

| compound | electronic spectra $\lambda_{max}$, nm ($\varepsilon$, $M^{-1}$ $cm^{-1}$) |
|---|---|
| $[Re(L^{1a})(L^{3a})]$ (**1a**) | 555 (12170), 464 (10873), 390(12776), 334 (17940), 270(22403) |
| $[Re(L^{1b})(L^{3b})]$ (**1b**) | 559 (9015), 468 (7785), 390 (9173), 337(14376), 270(18509) |
| $[Re(L^{2})(L^{4\bullet-})_2]$ (**2**) | 935 (5598), 602 (8458), 490 (20901), 290(18093) |

structural parameters and net spin densities for the computed ground states of the $[\mathbf{1b}]^+$, $[\mathbf{1b}]^{2+}$, $[\mathbf{2}]^+$, and $[\mathbf{2}]^{2+}$ are collected in Tables 2 and 3. The one electron oxidized monocationic complexes, $[\mathbf{1b}]^+$ and $[\mathbf{2}]^+$, have a doublet ground state, and the changes in net spin density indicate that the oxidation process is clearly ligand centered, although in the case of $[\mathbf{1b}]^+$, it is mainly localized on a single ligand ($L^{3b}$; Re = 0.1857, $L^{1b}$ = 0.0147, $L^{3b}$ = 0.7996; Figure S11, Supporting Information) while it is delocalized over the two aminophenoleto ligands in $[\mathbf{2}]^+$ (Re = −0.1523, $L^2$ = 0.0445, and $L^{4\bullet-}$ = 1.1078; Figure S12, Supporting Information). The two electron oxidized complexes $[\mathbf{1b}]^{2+}$ and $[\mathbf{2}]^{2+}$ have closed-shell singlet state structures, which again is consistent with the ligand centered redox process.

Overall, the oxidation states of the metal and the two ligands in compounds **1b** and **2** may be described as $[Re^{III}(L^{1b})^-(L^{3b})^{2-}]$ (**1b**) and $[Re^{III}(L^2)^-\{(L^4)^{\bullet-}\}_2]$ (**2**), respectively. The central Re(III) ion remains essentially invariant in the two redox processes $[\mathbf{1b/2}]^{1+/2}$, with all redox events localized on the ligands, which is in line with the EPR data.

All of the compounds **1** and **2** are freely soluble in nonpolar solvents like dichloromethane and chloroform, and their electronic spectra were recorded in dichloromethane solution. The experimental spectral results are collected in Table 5, and the corresponding spectra are displayed in Figure S13 (Supporting Information). The low intensity tail observed in the experimental spectrum compares well with the calculated value for the HOMO→LUMO transition at around 900−950 nm. The two midintensity peaks with transition maxima close to 550 (for **1b**) and 600 nm (for **2**) can be readily assigned to HOMO−1/HOMO−2→LUMO transitions, which are computationally predicted to appear at 592 and 606 nm, respectively. Several possible transitions were found to lie between 250 and 400 nm, which are assigned as the intraligand (ligand($\pi$)→ligand($\pi^*$)) charge transfer transition.[4]

## CONCLUSION

In conclusion, we have introduced an unprecedented type of multiple step redox process in Re-coordinated azoaromatic ligands. Attempts have been made to rationalize the formation of $H_2L^3$ from $HL^1$. Considering the products of all of the above-noted reactions together, one may think of the most simplest pathway of four electron reductive azo cleavage followed by oxidation of one of the imide fragments, leading to a symmetrical azo-aromatic ligand $[H_2L^3]$. It is thus concluded that dimetallic electron-rich mediators can cleave and reform azo bond(s) only on multidented azo-aromatics. The results have generated a scope of synthesizing otherwise inaccessible extended new azo-aromatic compounds by reactions of multimetal−carbonyls with polydentated (tri and higher) azoaromatic substrates. Our studies in this area are in progress.

## EXPERIMENTAL SECTION

**Materials.** $Re_2(CO)_{10}$ is an Aldrich reagent. The ligands $L^{1(a/b)}$ and $L^2$ were prepared by following the reported procedure.[17] All other chemicals were of reagent grade and used as received. Solvents were purified and dried prior to use.

**Instrumentation.** $^1H$ NMR spectra were taken on a Bruker Advance DPX 300 spectrometer, and $SiMe_4$ was used as the internal standard. Infrared spectra were obtained using a Perkin-Elmer 783 spectrophotometer. Cyclic voltammetry was carried out in 0.1 M $Bu_4NClO_4$ solutions using a three-electrode configuration (platinum working electrode, Pt counter electrode, Ag/AgCl reference) and a PC-controlled PAR model 273A electrochemistry system. The $E_{1/2}$ for the ferrocenium−ferrocene couple under our experimental conditions was 0.39 V. A Perkin-Elmer 240C elemental analyzer was used to collect microanalytical data (C, H, N). ESI mass spectra were recorded on a micro mass Q-TOF mass spectrometer (serial no. YA 263). EPR spectra in the X band were recorded with a JEOL JES-FA200 spectrometer.

**Syntheses.** *Reaction of $Re_2(CO)_{10}$ and $HL^{1(a/b)}$: Synthesis of $[Re(L^{1a})(L^{3a})]$ (**1a**).* A total of 100 mg of $Re_2CO_{10}$ (0.15 mmol) and 165 mg of $HL^{1a}$ (0.60 mmol) were heated at reflux for 4 days in *n*-octane. The color of the solution changed from red to pink during this period. The solution was filtered, which on evaporation produced a dark mass. The crude product was then loaded onto a preparative silica TLC plate for purification. Toluene was used as the eluent. Complex **1a** was separated on a TLC plate as a pink band with several other minor overlapping products. It was recrystallized by slow diffusion of a dichloromethane solution of the compound into hexane. Its yields and characterization data are as follows. Yield: 45%. IR (KBr, $cm^{-1}$): 1585 [$\nu$(C═N)], 1295 [$L^1\nu$(N═N)], 1285 [$L^2\nu$(N═N)]. ESI-MS, *m*/*z*: 822 $[MH]^+$. Anal. Calcd for $C_{41}H_{31}N_8Re$: C, 59.91; H, 3.80; N, 13.63. Found: C, 59.87; H, 3.82; N, 13.62. $^1H$ NMR (500 MHz, d6-DMSO, 300 K): $\delta$ 8.15 (d, 1H J = 8.5), 7.62 (d, 1H, J = 8.0 Hz), 7.53 (t, 1H, J1 = 7.0, J2 = 8.0 Hz), 7.41 (t, 1H, J 1= 7, J2 = 8.5 Hz), 7.30−7.28 (m, 2H), 7.16 (d, 1H, J = 8.0 Hz), 7.10−7.02 (m, 6H), 6.92 (t, 1H, J1 = 7.5, J2 = 7.5 Hz), 6.77 (t, 1H, J1 = 7.5, J2 = 7.5 Hz), 6.73−6.69 (m, 7H Hz), 6.65−6.60 (m, 3H), 6.55 (d, 1H, J = 8.0 Hz), 6.50 (t, 1H, J1 = 7.5, J2 = 7.5 Hz), 6.46 (t, 1H, J1 = 7.5, J2 = 7.0 Hz), 6.39 (d, 1H, J = 7.5 Hz), 6.30 (t, 1H, J1 = 6.5, J2 = 6.5 Hz), 6.23 (d, 1H, J= 8.0 Hz).

*Synthesis of $[Re(L^{1b})(L^{3b})]$ (**1b**).* This was synthesized following the same procedure as described for **1a**. Its yield and characterization data are as follows. Yield: 42%. IR (KBr, $cm^{-1}$): 1585 [$\nu$(C═N)], 1280 [$L^1\nu$(N═N)], 1275 [$L^2\nu$(N═N)]. ESI-MS, *m*/*z*: 864 $[MH]^+$. Anal. Calcd for $C_{44}H_{37}N_8Re$: C, 61.16; H, 4.32; N, 12.97. Found: C, 61.14; H, 4.34; N, 12.93. $^1H$ NMR (500 MHz, d6-DMSO, 300 K): $\delta$ 8.12 (d, 1H J = 8.0 Hz), 7.58 (d, 1H, J = 8.0 Hz), 7.50−7.49 (m, 2H), 7.42 (t, 1H, J1 = 7.5, J2 = 8.0 Hz), 7.34 (d, 1H, J = 8.5 Hz), 7.28 (d, 1H, J = 6.0 Hz), 7.14 (d, 2H, J = 8.0 Hz), 7.08 (d, 1H, J = 8.0 Hz), 7.02 (t, 1H, J1= 8.0, J2= 8.5 Hz), 6.77 (d, 1H, J = 7.5 Hz), 6.73−6.67 (m, 6H), 6.60 (t, 1H, J1= 7.5, J2=7.5), 6.53−6.49 (m, 5H), 6.43 (t, 1H, J1 = 7.5, J2 = 8 Hz), 6.27 (t, 1H, J1= 6.5, J2= 7.0), 6.21 (d, 1H, J= 6.0 Hz), 6.13 (d, 1H, J = 8.0 Hz).

*Reaction of $Re_2(CO)_{10}$ and $HL^2$: Synthesis of $[Re(L^2)\{(L^4)^{\bullet-}\}_2]$ (**2**).* A total of 100 mg of $Re_2CO_{10}$ (0.15 mmol) and 190 mg of $HL^2$ (0.61 mmol) were heated at reflux for 96 h in *n*-octane. The color of the solution changed from orange to dull green during this period. The solution was filtered, which on evaporation produced a dark mass. The crude product was then loaded onto a preparative silica TLC plate for purification. Chloroform was used as the eluent. Complex **2** was separated on a TLC plate as a dull green band as a major product with some other minor overlapping products. It was recrystallized by slow evaporation of a methanol−dichloromethane solvent mixture of the


dx.doi.org/10.1021/ic201200r |*Inorg. Chem.* 2011, 50, 7886–7893

complex. Its yields and characterization data are as follows. Yield: 60%. IR (KBr, $cm^{-1}$): 1580 [$\nu$(C═N)], 1260 [$L^1\nu$(N═N)]. ESI-MS, $m/z$: 936 $[MH]^+$. Anal. Calcd for $C_{47}H_{66}N_5O_3Re$: C, 60.36; H, 7.11; N, 7.49. Found: C, 60.32; H, 7.15; N, 7.45. $^1H$ NMR (500 MHz, $CDCl_3$, 300 K): $\delta$ 9.32 (s, 1H (N−H)), 8.98 (s, 1H (N−H)), 7.84 (s, 1H), 7.79−7.58 (m, 2H), 7.48 (t, 1H, J1 = 9, J2 = 8.5 Hz), 7.41 (t, 1H, J1 = 8.5, J2 = 8.0 Hz), 7.06 (s, 1H), 6.98 (s, 1H), 6.78 (s, 1H), 6.73 (s, 1H Hz), 6.66 (s, 1H Hz), 1.45−1.23 (s, 54H).

*Reaction of $Re(CO)_5Cl$ and $HL^1$: Synthesis of [Re(pap)$(CO)_3$Cl] (**3**).* A total of 100 mg of $Re(CO)_5Cl$ (0.27 mmol) and 150 mg of $HL^1$ (0.54 mmol) was heated at reflux for 3 days in *n*-octane. The color of the solution changed from red to deep blue during this period. The solution was filtered, which on evaporation produced a dark mass. Recrystallization of the crude product from dichloromethane/hexane solution produced complex **3**. Its yield and characterization data are as follows. Yield: 75%. IR (KBr, $cm^{-1}$): 1580 [$\nu$(C═N)], 1290 [L$\nu$(N═N)], 1905 [$\nu$(C≡O)]. ESI-MS, $m/z$: 489 $[MH]^+$. Anal. Calcd for $C_{14}H_9ClN_3O_3Re$: C, 34.39; H, 1.86; N, 8.59. Found: C, 34.37; H, 1.89; N, 8.58.

*Reaction of $Re_2(CO)_{10}$ and $L^5$: Synthesis of [Re($L^{5\bullet-}$)$_2$$(CO)_2$] (**4**).* A total of 100 mg of $Re_2CO_{10}$ (0.15 mmol) and 165 mg of $HL^{1a}$ (0.61 mmol) were heated at reflux for 96 h in *n*-octane. The color of the solution changed from orange to deep blue during this period. The crude complex was crystallized from a hot *n*-octane solution of the reaction mixture. Its yield and characterization data are as follows. Yield: 75%. IR (KBr, $cm^{-1}$): 1195 [$\nu$(N═N)]; 1875, 1940 [$\nu$(C≡O)]. ESI-MS, $m/z$: 791 $[MH]^+$. Anal. Calcd for $C_{36}H_{28}N_8O_2Re$: C, 54.67; H, 3.57; N, 14.17. Found: C, 54.63; H, 3.60; N, 14.14.

**EPR Spectral Studies.** The one electron oxidized complexes $[\mathbf{1}]^+$ and $[\mathbf{2}]^+$, generated by exhaustive electrolysis of the respective complexes **1** and **2** at 0.65 and 0.7 V, respectively, in $CH_2Cl_2$/0.1 M TBAP, were immediately dipped into liquid nitrogen, and the resulting frozen solutions were used for the EPR measurements at 77 K. The applied potential for the two electron oxidized complexes $[\mathbf{1}]^{2+}$ and $[\mathbf{2}]^{2+}$ are 1.0 and 1.2 V, respectively.

**Crystallography.** Crystallographic data for compounds **1b**, **2**, and **3** are collected in Table S-1 (Supporting Information). Suitable X-ray quality crystals of these are obtained as follows: **1b**, by slow evaporation of a dichloromethane−hexane solvent mixture of the compound; **2**, by slow evaporation of a methanol−dichloromethane solution of the compound; and **3**, by slow evaporation of dichloromethane−hexane solution of the compound.

All data were collected on a Bruker SMART APEX-II diffractometer, equipped with graphite monochromated Mo K$\alpha$ radiation ($\lambda$ = 0.71073 Å), and were corrected for Lorentz-polarization effects. **1b**: A total of 43 806 reflections were collected, of which 9605 were unique ($R_{int}$ = 0.063), satisfying the ($I > 2\sigma(I)$) criterion, and were used in subsequent analysis. **2**: A total of 26 869 reflections were collected, of which 8364 were unique ($R_{int}$ = 0.057). **3**: A total of 16 378 reflections were collected, of which 2484 were unique ($R_{int}$ = 0.082).

The structures were solved by employing the SHELXS-97 program package[18] and were refined by full-matrix least-squares based on $F^2$ (SHELXL-97).[19] All hydrogen atoms were added in calculated positions.

**Computational Details.** All calculations described in this paper were performed using density functional theory as implemented in the Gaussian 03 package.[20] Full geometry optimizations were performed without symmetry constraints. The vibrational frequency calculations were performed to ensure that the optimized geometries represent the local minima and that there are only positive Eigen values. The hybrid B3LYP exchange-correlation functional was used in conjunction with the SDD basis set with effective core potential for the Re atom and the 6-31G(d) basis set for C, H, N, and O atoms. GaussSum[21] was used to calculate the fractional contributions of various groups to each molecular orbital.

## ■ ASSOCIATED CONTENT

**Supporting Information.** Experimental and characterization details, X-ray crystallographic files in CIF format, and ORTEP and respective atom numbering schemes for **1**−**3** are provided. This material are available free of charge via the Internet at http://pubs.acs.org.

## ■ AUTHOR INFORMATION

**Corresponding Author**
*E-mail: icsg@iacs.res.in.

## ■ ACKNOWLEDGMENT

The research was supported by Department of Science and Technology, New Delhi (Project: SR/S1/IC/0031/2010). Crystallography was performed at the DST-funded National Single Crystal Diffractometer Facility at the Department of Inorganic Chemistry, IACS. N.D.P. and S.S. thank the Council of Scientific and Industrial Research for fellowship support.

## ■ REFERENCES

(1) (a) *Handbook of Metathesis*; Grubbs, R. H., Ed.; Wiley-VCH: Weinheim, Germany, 2003; Vols 1−3. (b) For a major account of Ru metathesis catalysts, see: Nguyen, S. T.; Trnka, T. M. In *Handbook of Metathesis*; Grubbs, R. H., Ed.; Wiley-VCH: Weinheim, Germany, 2003; Vol. 1, chapter 1.6. (c) Trnka, T. M; Grubbs, R. H. *Acc. Chem. Res.* **2001**, *34*, 18 and references therein. (d) Astruc, D. *New J. Chem.* **2005**, *29*, 42 and references therein.

(2) (a) Basset, J.-M.; Copéret, C.; Soulivong, D.; Taoufik, M.; Cazat, J. T. *Acc. Chem. Res.* **2010**, *43*, 323. (b) Alcaide, B.; Almendros, P.; Luna, A. *Chem. Rev.* **2009**, *109*, 3817.

(3) (a) Grirrane, A.; Corma, A.; García, H. *Science* **2008**, *322*, 1661. (b) Zhang, C.; Jiao, N. *Angew. Chem., Int. Ed.* **2010**, *49*, 6174.(c) Hunger, K. *industrial dyse: Chemistry, properties, Applications*; Wiley-VCH: Weinheim, Germany, 2003. (d) Andersosn, R. G.; Nickless, G. *Analyst* **1967**, *92*, 25. (e) Ashutosh, P. N. D.; Mehrotra, J. K. *Colourage* **1979**, *26*, 25. (f) Athey, R. D., Jr. *Eur. Coatings J.* **1998**, *3*, 146. (g) Sheppard, C. S. *Encycl. Polym. Sci. Eng.* **1985**, *2*, 143. (h) Hoult, J. R. S. *Drugs* **1986**, *97*, 2939. (i) Sandborn, W. J. *Am. J. Gastroenterol.* **2002**, *97*, 2939.(j) Cation, S. C.; Farris, E. *Consise Encyclopedia of Chemical Technilogy*; Wiley: New York, 1985.

(4) (a) Paul, N. D.; Samanta, S.; Goswami, S. *Inorg. Chem.* **2009**, *49*, 2649. (b) Sanyal, A.; Banerjee, P.; Lee, G.-H.; Peng, S.-M.; Hung, C.-H.; Goswami, S. *Inorg. Chem.* **2004**, *43*, 7456. (c) Sanyal, A; Chatterjee, S; Castiñeiras, A; Sarkar, B; Singh, P; Fiedler, J; Záliš, S; Kaim, W; Goswami, S. *Inorg. Chem.* **2007**, *46*, 8584. (d) Samanta, S.; Singh, P.; Fiedler, J.; Záliš, S.; Kaim, W.; Goswami, S. *Inorg. Chem.* **2008**, *47*, 1625. (e) Sanyal, A.; Banerjee, P.; Lee, G.-H.; Peng, S.-M.; Hung, C.-H.; Goswami, S. *Inorg. Chem.* **2004**, *43*, 7456.

(5) Sarkar, B.; Patra, S.; Fiedler, J.; Sunoj, R. B.; Janardanan, D.; Lahiri, G. K.; Kaim, W. *J. Am. Chem. Soc.* **2008**, *130*, 3532 and references therein. (g) Doslik, N.; Sixt, T.; Kaim, W. *Angew. Chem., Int. Ed.* **1998**, *37*, 2403. (h) Kaim, W. *Coord. Chem. Rev.* **2001**, *219*, 463.

(6) (a) Sinan, M.; Panda, M.; Banerjee, P.; Shinisha, C. B.; Sunoj, R. B.; Goswami, S. *Org. Lett.* **2009**, *11*, 3219 and references therein.

(7) (a) Laplaza, C. E.; Cummins, C. C. *Science* **1995**, *268*, 861. (b) Sadique, R. A.; Gregory, A. E.; Brennessel, W. W.; Holland, L. *J. Am. Chem. Soc.* **2007**, *129*, 8112. (c) Lentz, M. R.; Vilardo, J. S.; Lockwood, M. A.; Fanwick, P. E.; Rothwell, I. P. *Organometallics* **2004**, *23*, 329 and references therein. (d) Peters, R. G.; Warner, B. P.; Burns, C. J. *J. Am. Chem. Soc.* **1999**, *121*, 5585 and references therein. (e) Evans, W. J.; Kozimor, S. A.; Ziller, J. W. *Chem. Commun.* **2005**, 4681. (f) Ohki, Y.; Takikawa, Y.; Hatanaka, T.; Tatsumi, K. *Organometallics* **2006**, *25*, 3111. (g) Pan, C.-L.; Chen, W; Song, S.; Zhang, H.; Li, X. *Organometallics*

**2009**, *48*, 6344. (h) Lahiri, G. K.; Goswami, S.; Falvello, L.; Chakravorty, A. *Inorg. Chem.* **1987**, *26*, 3365. (i) Ghosh, A. K.; Majumdar, P.; Falvello, R. L.; Mostafa, G.; Goswami, S. *Organometallics* **1999**, *18*, 5086.

(8) Zarkesh, R. A.; Ziller, J. W.; Heyduk, A. F. *Angew. Chem., Int. Ed.* **2008**, *47*, 4715.

(9) Xu, L.; Setyawati, I. A.; Pierreroy, J.; Pink, M.; Young, V. G., Jr.; Patrick, B. O.; Rettig, S. J.; Orvig, C. *Inorg. Chem.* **2000**, *39*, 5958 and references therein.

(10) (a) Saha, A.; Ghosh, A. K.; Majumder, P.; Mitra, K. N.; Mondal, S.; Rajak, K. K.; Falvello, L. R.; Goswami, S. *Organometallics* **1999**, *18*, 3772. (b) Saha, A.; Majumder, P.; Goswami, S. *J. Chem. Soc., Dalton Trans.* **2000**, *11*, 1703. (c) Saha, A.; Majumder, P.; Peng, S.-M.; Goswami, S. *Eur. J. Inorg. Chem.* **2000**, *12*, 2631.

(11) (a) Cotton, F. A.; Duraj, S.; Roth, W. *J. Am. Chem. Soc.* **1984**, *106*, 4749. (b) Hill, J. E.; Profilet, R. D.; Fanwick, P. E.; Rothwell, I. P. *Angew. Chem., Int. Ed. Engl.* **1990**, *29*, 664. (c) Hill, J. E.; Fanwick, P. E.; Rothwell, I. P. *Inorg. Chem.* **1991**, *30*, 1143. (d) Zambrano, C. H.; Fanwick, P. E.; Rothwell, I. P. *Organometallics* **1994**, *13*, 1174.

(12) Sengupta, S.; Panda, B. K. *Transition Met. Chem.* **2005**, *30*, 426.

(13) Saha, A.; Das., C.; Goswami, S.; Peng, S.-M. *Indian J. Chem., Sect. A* **2001**, *40A*, 198.

(14) Paul, N. D.; Krämer, T.; Mcgrady, J. E.; Goswami, S. *Chem. Commun* **2010**, *46*, 7124.

(15) (a) Chun, H.; Bill, E.; Weyhermüller, T.; Wieghardt, K. *Inorg. Chem.* **2003**, *42*, 5612 and reference therein. (b) Sproules, S.; Benedito, F. L.; Bill, E.; Weyhermüller, T.; George, S. D.; Wieghardt, K. *Inorg. Chem.* **2009**, *48*, 10926. (c) Bhattacharya, S.; Gupta, P.; Basuli, F.; Pierpont, C. G. *Inorg. Chem.* **2002**, *41*, 5810.

(16) (a) Das, C.; Ghosh, A. K.; Hung, C.-H.; Lee, G.-H.; Peng, S.-M.; Goswami, S. *Inorg. Chem.* **2002**, *41*, 7125. (b) Das, C.; Saha, A.; Hung, C.-H.; Lee, G.-H.; Peng, S.-M.; Goswami, S. *Inorg. Chem.* **2003**, *42*, 198. (c) Kamar, K. K.; Saha, A.; Castiñeiras, A.; Hung, C.-H.; Goswami, S. *Inorg. Chem.* **2002**, *41*, 4531.

(17) Campbell, N.; Henderson, A. W.; Taylor, D. *J. Chem. Soc.* **1953**, 1281. (b) Anderson, R. G.; Nickless, G. *Anal. Chim. Acta* **1967**, *39*, 469.

(18) Sheldrick, G. M. *Acta Crystallogr., Sect. A* **1990**, *46*, 467.

(19) Sheldrick, G. M. *SHELXL 97*; University of Göttingen; Göttingen, Germany, 1997.

(20) Frisch, M. J. et al. *Gaussian 03*; Gaussian, Inc.: Wallingford, CT, 2004.

(21) O'Boyle, N. M.; Tenderholt, A. L.; Langner, K. M. *J. Comput. Chem.* **2008**, *29*, 839.